

Multiscale Oil Slick Segmentation with Markov Chain Model

Grégoire MERCIER*, Stéphane DERRODE†, Wojciech PIECZYNSKI‡,
Jean-Marc LE CAILLEC* and René GARELLO*

*GET - ENST Bretagne, dpt ITI, CNRS FRE 2658 TAMCIC, team TIME.
Technopole Brest-Iroise, CS 83818; 29238 Brest cedex - France

†ENSPM, Laboratoire Fresnel (UMR 6133), team GSM.

Domaine universitaire de Saint Jérôme, 13013 Marseille Cedex 20 - France

‡GET - INT, dpt CITI, 9, Rue Charles Fourier, 91011 Evry Cedex - France

Abstract—A Markov chain model is applied for the segmentation of oil slicks acquired by SAR sensors. Actually, oil slicks have specific impact on ocean wave spectra. Initial wave spectra may be characterized by three kinds of waves, big, medium and small, which correspond physically to gravity and gravity-capillary waves. The increase of viscosity due to the presence of oil damps gravity-capillary waves. This induces a damping of the backscattering to the sensor, but also a dampening of the energy of the wave spectra. Thus, local segmentation of wave spectra may be achieved by the segmentation of a multiscale decomposition of the original SAR image.

In this work, the unsupervised segmentation is achieved by using a vectorial extension of the Hidden Markov Chain (HMC) model. Parameters estimation is performed using the general Iterative Conditional Estimation (ICE) method. The problem of estimating multi-dimensional and non-Gaussian densities is solved by using a Principal Component Analysis (PCA). The algorithm has been applied on an ERS-PRI image. It yields interesting segmentation results with a very limited number of false alarms. Also, the multiscale segmentation proved to be an interesting alternative to classify marginal or degraded slicks.

I. INTRODUCTION

Oil slicks may be found all over the Ocean and play a relevant role in large- and short-scale phenomena such as Global Change by modifying the delicate air-sea balance or the local pollution by the interaction with the marine ecosystems. Detection and characterization of oil spills caused by accidental or intentional emission may be achieved by remote sensing, especially Synthetic Aperture Radar (SAR) that can be used independently from the day-light and weather conditions.

SAR is sensitive to sea surface thanks to the presence of short-waves and wind is the most important generator of waves. Capillary waves rise first when the wind blows over the sea surface. Basically, the wavelength λ of the capillary waves are inferior to 5mm and satisfy the dispersion relationship $\omega^2 = \frac{\tau}{\rho} \kappa^3$ where τ is the surface tension, ρ the water density, κ the surface wavenumber and $\omega = \frac{2\pi}{\lambda}$. If the wind still induces excitation, the capillary waves transfer energy to waves of longer wavelength and so on until an equilibrium with long (several hundred meters length), intermediate (tens of meters length) and short (less than a meter) waves. Gravity waves obey the following dispersion equation $\omega^2 = g\kappa$, where g

is the gravity acceleration. The classical dispersion relation that describes the sea surface wave spectrum which may be observed by remote sensing follows:

$$\omega^2 = g\kappa + \frac{\tau}{\rho} \kappa^3.$$

The presence of oil on the water reduces air-sea interaction and the main observable phenomena is the dampening of the capillary waves. This reduces the backscattering of the slick and then yields a darker area in the SAR image. Hence, most of the algorithms dedicated to the *detection* of oil slicks are based on contrast ratio [1].

Unfortunately, dark area may also be induced by several phenomena such as lack of wind, upwellings... and it is necessary to predict the effects of slicks on sea surface and also SAR images [2]. According to the Marangoni theory, dampening of the capillary waves induces a variation of the surface spectrum for wavelength lower than 1m, due to elasticity and viscosity of the oil. Moreover, non-linear wave-wave interactions spread the energy in order to fill in dips of the spectrum and reduce the energy of the peaks.

Finally, oil slicks induce on the one hand a dampening of the capillary wave that is observable via darker area on SAR images which is useful for detection. On the other hand, slicks induce also a spreading of the sea surface wave spectrum. In this study, we propose an algorithm for detecting local variations of the wave spectrum. Actually, the algorithm is based on a multiscale analysis to represent observation as a local multiscale description of the oceanic waves, and on a texture segmentation method that is based on the estimation of mixtures of probability density functions (pdf) that are observed over the multiscale representation.

II. MULTISCALE ANALYSIS

The remotely sensed observation (Y) is first decomposed into multiscale analysis in order to outline its local texture characteristics at different wavelengths.

Wavelets have been widely studied and characterized for texture analysis. The choice of the mother wavelet has a major impact on texture characterization [3]. It is required to use symmetric filters with enough number of vanishing moments and regularity in the critically sampled filter banks.

For this multiscale analysis, the wavelet used has been defined in [4]. The set of filters is built to guaranty a good localization of multiscale edges. Only two wavelet filters are required:

$$\theta(x, y) = \theta(x)\theta(y)$$

$$\psi^{\text{hori}}(x, y) = \frac{\partial\theta(x, y)}{\partial x} \quad \text{and} \quad \psi^{\text{vert}}(x, y) = \frac{\partial\theta(x, y)}{\partial y} \quad (1)$$

Where, the primitive $\theta(\cdot)$ is a cubic spline with Fourier transform given by:

$$\widehat{\theta}(\omega) = \left(\frac{\sin(\omega/4)}{\omega/4} \right)^3. \quad (2)$$

Note that the multiscale analysis of an image yield two subbands of wavelet coefficients at each decomposition $\ell \in [1, L]$. Observation Y is then decomposed, by iterative convolutions with filters defined with $\theta(\cdot)$, $\psi^{\text{hori}}(\cdot)$ and $\psi^{\text{vert}}(\cdot)$, to yield the vector $\mathbf{Y} = (\Theta_L, \Psi_{L-1}^{\text{hori}}, \Psi_{L-1}^{\text{vert}}, \dots, \Psi_1^{\text{hori}}, \Psi_1^{\text{vert}})^t$.

III. HIDDEN MARKOV CHAIN MODEL

In the context of HMC model, the remote sensing data is considered as a *noisy* observation from which the segmentation has to be found. The 2D observation is first transformed into a 1D chain through a Hilbert-Peano scan on the image [5]. When this observation is of vector value, the Hilbert-Peano scan is applied spatially in order to yield a chain that contains each pixel (*i.e.* $(\Theta_L, \Psi_{L-1}^{\text{hori}}, \Psi_{L-1}^{\text{vert}}, \dots, \Psi_1^{\text{hori}}, \Psi_1^{\text{vert}})^t$) along the scan.

A. Overview of the scalar case

It is considered that observations y , which are the pixels of the image, are the noisy realizations of a random process X that takes its values in $\Omega = \{\omega_1, \omega_2, \dots, \omega_K\}$, K being the number of classes expected for the segmentation. Several methods may be considered when the link between observation Y and segmentation X (*i.e.* $P(X, Y)$) is known. If it is not the case, $P(X, Y)$ has first to be estimated. Here, it is supposed that X is a stationary Markovian process and parameters estimation is achieved using ICE algorithm [6]. The ICE procedure is based on the conditional estimation of some estimators from the complete data (x, y) . It is an iterative method which produces a sequence of estimations θ^q of parameters θ as follows: 1) initialize θ^0 ; 2) compute $\theta^{q+1} = \mathbb{E} \left[\hat{\theta}(X, Y) | Y = y \right]$, where $\hat{\theta}(X, Y)$ is an estimator of θ . Usually, ICE is stopped when $\theta^{q+1} \approx \theta^q$. The parameters θ to estimate are of two kinds:

- 1) the set Π that characterizes the stationary Markov Chain X : the initial probability vector $\pi = (P(X = \omega_1), \dots, P(X = \omega_K)) = (\pi_{\omega_1}, \dots, \pi_{\omega_K})$ and the transition matrix A of components $P(X = \omega_k, X = \omega_l) = a_{w_k, w_l}$ ($1 \leq k, l \leq K$).

In an ICE iteration, the expectation of those parameters can be evaluated analytically along the Hilbert-Peano chain by using the normalized Baum's Forward and Backward probabilities [7].

- 2) the mixture parameters set Δ that characterizes observation for each class ω_k : $P(Y|X = \omega_k)$ of pdf f_{ω_k} . In the Gaussian case, Δ is composed of means and variances; by using the Pearson's system of distributions [8], Δ needs the four first moments for each pdf. For those parameters, θ^{q+1} is not tractable. But it can be estimated by empirical mean of several estimations according to $\theta^{q+1} = \frac{1}{L} \sum_{\ell} \hat{\theta}(x^{\ell}, y)$, where x^{ℓ} is an *a posteriori* realization of X conditionally on Y .

B. Integration of multi-component observations

In the case of the segmentation of the multiscale analysis, observation Y is becoming a multi-dimensional random variable \mathbf{Y} of dimension $M = 2L + 1$.

Then, pdf $f_{\omega_k}(\cdot)$ are becoming M -dimensional distributions to be estimated. Although not independent, the wavelets coefficients are rather decorrelated along the scales and we consider that they can be estimated by considering M estimation of independent 1D pdf. Thus pdf $f(\mathbf{y})$ is considered as a M -dimensional distribution with self-independent component, *i.e.* $f(\mathbf{y}) = \prod_{m=1}^M f_m(y_m)$. In order to estimate the mixture pdf $f_{\omega_k}(\mathbf{y})$, a Principal Component Analysis (PCA) is applied on the data at each iteration of the ICE procedure. Although, not rigorously independent since an ACP is applied, $f_{\omega_k}(\mathbf{y})$ is also considered as a M -dimensional distribution with self-independent component, *i.e.* $f_{\omega_k}(\mathbf{y}) = \prod_{m=1}^M f_{m, \omega_k}(y_m)$.

It should be possible to apply Independent Component Analysis (ICA) for each estimation of $f_{\omega_k}(\mathbf{y})$ at each iteration of the ICE algorithm; but ICA is a non-orthogonal projection that tends to yield multi-modal distributions (actually, non-gaussianity acts as an independence criteria) that makes ICA procedure not converging.

Finally, the restoration is achieved by using the Maximum a Posteriori Mode (MPM) Bayesian segmentation rule.

C. Pdf modelization

The image Θ_L is a coarse approximation of the initial observation Y , then its overall pdf is a smooth restitution of the initial $f(y)$. The estimation of a generalized mixture of laws included in this pdf may be achieved by considering distributions defined within the Pearson's system of distributions [8] which include Gaussian, Gamma and Beta distributions. The four first moments have to be estimated in order to characterize the laws and the parameters of the pdf of Θ_L .

The images $\Psi_{\ell}^{\text{h}} \text{ or } \Psi_{\ell}^{\text{v}}$ come from the wavelet decomposition and experiments [9] show that a good pdf approximation for the marginal density of wavelet coefficients at a given subband may be achieved by the Generalized Gaussian Density (GGD) defined by [10]. Then, mixture pdf $f_{m, \omega_k}(y_m)$ at a given scale is defined by:

$$p(x; \mu, \alpha, \beta) = \frac{\beta}{2\alpha\Gamma(\frac{1}{\beta})} e^{-\left(\frac{|x-\mu|}{\alpha}\right)^{\beta}},$$

where μ, α, β are the mean, scale and shape parameters that are estimated by using maximum likelihood estimator.

The pdf of the transform observation \mathbf{Y} is considered as a generalized mixture of multi-dimensional laws that are characterized with the 4 first moments for Θ_L and the 3 parameters of GGD for the $2L$ subbands Ψ_ℓ^v or h .

IV. EXPERIMENTS

Multi-component Markov chain model has been applied to ERS-SAR image acquired over Mediterranean Sea during oil spill. A first step may be applied to the original image in order to achieve the *detection* of oil slicks. For detecting slicks, we applied an algorithm that is modified from the one presented earlier. Actually, the multi-scale analysis is replaced by a multi-resolution analysis achieved by wavelet packet transform with the 9/7 mother wavelet. This multi-resolution analysis allow to process images of large size. The result of detection is presented on Fig. 1.

Let's focus now on a small part of the image where oil slick has been detected with no ambiguity in order to *characterize* the dark area. Several comparison have been achieved and shown in Fig. 2. On images -b- and -c-, a characterization by a simple threshold or a Markov chain applied directly on the image show a lot of false alarms and miss-detections. But the segmentation that is given by the Markov chain applied on the wavelet coefficients -d- is more interesting. First, the result is regularized and greatly reduces the number of false alarms. Also, it appears that the class on grey acts as an intermediate between oil and water. It may be characteristic of mixture or marginal slick area.

V. CONCLUSION

An oil slick segmentation procedure has been developed in order to detect the spatial variations of the surface wave spectra. The segmentation is based on a multiscale analysis of the observed data and then a texture segmentation based on a multi-component Markov chain. It appears that a segmentation based on the behavior of the surface wave spectra allows to characterize (by the parameters of the pdf found) each class and then to better characterize the meaning of the dark area on SAR images.

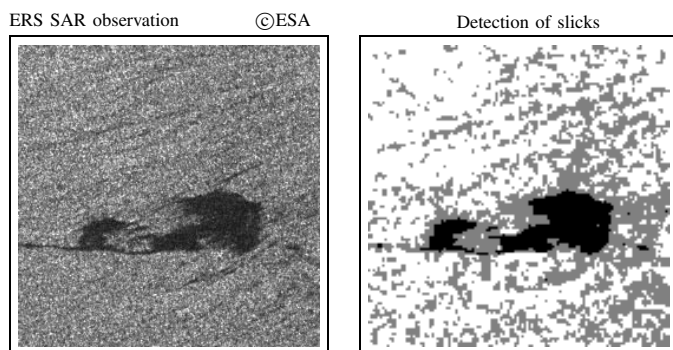


Fig. 1. Original observation and detection of oil slicks based on a wavelet packet analysis and a Markov chain model applied on the wavelet coefficients.

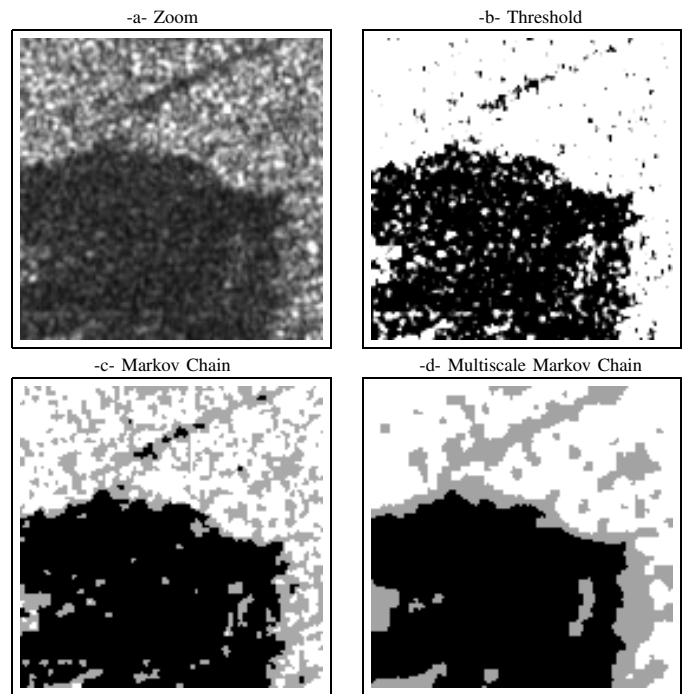


Fig. 2. Zoom on a detected oil slick and results of segmentation.

ACKNOWLEDGMENT

Authors would like to thank Fanny ARDHUIN from ENST Bretagne for her helpful and valuable comments and suggestions.

REFERENCES

- [1] T. Kanaa, E. Tonye, V. Onana, G. Mercier, R. Garello, and J. Mvogo, "Detection of oil slick signatures in SAR images by fusion of hysteresis thresholding responses," in *IGARSS*, 2003.
- [2] G. Franceschetti, A. Iodice, D. Riccio, G. Ruello, and R. Siviero, "SAR raw signal simulation of oil slicks in ocean environments," *IEEE transactions on geoscience and remote sensing*, vol. 40, no. 9, pp. 1935–1949, September 2002.
- [3] A. Mojsilović, M. Popović, and D. Rachov, "On the selection of an optimal wavelet basis for texture characterization," *IEEE Transactions on Image Processing*, vol. 9, no. 12, pp. 2043–2050, December 2000.
- [4] S. Mallat and S. Zhong, "Characterization of signals from multiscale edges," *IEEE transactions on Pattern Analysis and Machine Intelligence*, vol. 14, no. 7, pp. 710–732, July 1992.
- [5] N. Giordana and W. Pieczynski, "Estimation of generalized multisensor hidden Markov chain and unsupervised image segmentation," *IEEE Trans. Pattern Anal. Machine Intell.*, vol. 19, no. 5, pp. 465–475, May 1997.
- [6] W. Pieczynski, "Statistical image segmentation," *Mach. Graph. and Vis.*, vol. 1, pp. 261–268, 1992.
- [7] P. Devijver, "Baum's forward-backward algorithm revisited," *Pattern Recognition Letter*, vol. 3, pp. 369–373, 1985.
- [8] S. Derrode, G. Mercier, J.-M. LeCaillec, and R. Garello, "Estimation of sea-ice SAR clutter statistics from Pearson's system of distributions," in *IGARSS*, 2001.
- [9] S. Mallat, "A theory for multiresolution signal decomposition: the wavelet representation," *IEEE transactions on Pattern Analysis and Machine Intelligence*, vol. 11, no. 17, pp. 674–693, July 1989.
- [10] G. V. de Wouwer, P. Scheunders, and D. V. Dyck, "Statistical texture characterization from discrete wavelet representation," *IEEE Transactions on Image Processing*, vol. 8, no. 4, pp. 592–598, April 1999.